DISCUSSION

The experiments described in the preceding section have demonstrated that, with Ge(Li) detectors, the resonant scattering of bremsstrahlung can be successfully applied to the heaviest stable nuclei. In these nuclei, any level in the range of 1.5 to 4.5 MeV excitation energy can be observed with this method, provided $gA\Gamma_0^2/\Gamma \gtrsim 5$ meV, where A is the abundance of the isotope in the scatterer. This means that for $g = A = \Gamma_0/\Gamma = 1$, all levels having lifetimes shorter than $\sim 10^{-13}$ sec can be studied without regard to the multipole character.

As far as the nucleus Bi^{209} is concerned, resonant scattering from the $\frac{9}{2}+$ and $\frac{11}{2}+$ members of the 2.6-MeV septuplet has been observed. From the summary given in Table II it is concluded that the measured $E1$ strengths to the ground state are well reproduced by the particle-vibration coupling model in

the form used by Hamamoto,[10] with an effective charge $e_{\rm eff}^2(E1) = 0.05$.

Note added in proof. The results of another Coulomb excitation experiment involving the Bi^{209} septuplet have recently been reported by J. W. Hertel, D. G. Fleming, J. P. Schiffer, and H. E. Gove, Phys. Rev. Letters **23**, 488 (1969).

ACKNOWLEDGMENTS

The author is indebted to Dr. I. Hamamoto and to Dr. R. Broglia and his co-workers for the communication of results prior to publication. He wishes to thank Dr. S. Fallieros for directing his attention to the problem and for discussions; Dr. P. Federman for advice on theoretical points; and Dr. V. K. Rasmussen and Dr. C. P. Swann for help with experimental matters.

[10] I. Hamamoto, Nucl. Phys. **A135**, 576 (1969).

Nuclear-Structure Studies of ^{91,92,93,95,97}Nb and ^{94}Mo with the (^{3}He, d) Reaction*†

M. R. Cates,‡ J. B. Ball, and E. Newman

Oak Ridge National Laboratory, Oak Ridge, Tennessee 37830

(Received 1 July 1969)

The structure of the low-lying levels of ^{91,92,93,95,97}Nb and ^{94}Mo was investigated with the proton-stripping (^{3}He, d) reaction on targets of ^{90,91,92,94,96}Zr and ^{93}Nb. The incident energy was 30.9 MeV for the ^{91,92}Zr and ^{93}Nb reactions and 24.7 MeV for the ^{94,96}Zr reactions. The ^{90}Zr reaction was studied at both energies. The experimental angular distributions are compared with local zero-range distorted-wave Born-approximation calculations, and spin, parity, and spectroscopic factors are deduced. The extracted spectroscopic factors are used to establish the proton configurations of the target ground states. The observed levels and spectroscopic factors are compared with shell-model predictions based on an ^{88}Sr core. A surprising deviation from results of the simple shell-model calculations is observed for the relative transfer strengths to the two lowest 2+ levels in ^{94}Mo.

I. INTRODUCTION

NUCLEI in the $A = 90$ region have been the subject of a considerable number of theoretical and experimental studies in recent years. The general conclusion of these investigations is that the low-lying levels for these nuclei can be described reasonably well within the framework of a shell model restricted to only a few active orbitals.[1–6]

Much of the detailed information on the nuclei in this mass region has been obtained by the study of single-nucleon transfer direct reactions. Among the recent studies of neutron transfer reactions are the (d, p) work of Cohen,[7] Cohen and Chubinski,[8] Sheline et al.,[9] and Dickens and Eichler[10]; the (p, d) work of Sweet et al.,[11] Ball and Fulmer,[12] and Stautberg et al.[13]; the $(^3$He, $\alpha)$ work of Rundquist et al.,[14] Fou et al.,[15]

[1] B. F. Bayman, A. S. Reiner, and R. K. Sheline, Phys. Rev. **115**, 1627 (1959).

[2] I. Talmi and I. Unna, Nucl. Phys. **19**, 225 (1960).

[3] K. H. Bhatt and J. B. Ball, Nucl. Phys. **63**, 286 (1965).

[4] N. Auerbach and I. Talmi, Nucl. Phys. **64**, 458 (1965).

[5] J. Vervier, Nucl. Phys. **75**, 17 (1965).

[6] S. Cohen, R. D. Lawson, M. H. Macfarlane, and M. Soga, Phys. Letters **10**, 195 (1964).

[7] B. L. Cohen, Phys. Rev. **125**, 1358 (1962).

[8] B. L. Cohen and O. V. Chubinsky, Phys. Rev. **131**, 2184 (1963).

[9] R. K. Sheline, R. T. Jernigan, J. B. Ball, K. H. Bhatt, Y. E. Kim, and J. Vervier, Nucl. Phys. **61**, 342 (1965).

[10] J. K. Dickens and E. Eichler, Nucl. Phys. **A101**, 408 (1967).

[11] R. F. Sweet, K. H. Bhatt, and J. B. Ball, Phys. Letters **8**, 131 (1964).

[12] J. B. Ball and C. B. Fulmer, Phys. Rev. **172**, 1199 (1968).

[13] M. M. Stautberg, R. R. Johnson, J. J. Kraushaar, and B. W. Ridley, Nucl. Phys. **A104**, 67 (1967).

[14] D. E. Rundquist, M. K. Brussel, and A. I. Yavin, Phys. Rev. **168**, 1296 (1968).

[15] C. M. Fou, R. M. Zurmuhle, and J. M. Joyce, Phys. Rev. **155**, 1248 (1967).

TABLE I. Nominal thicknesses and isotopic abundances of targets.

Target	Approximate thickness (mg/cm^2)	Abundances (at.%)				
		^{90}Zr	^{91}Zr	^{92}Zr	^{94}Zr	^{96}Zr
^{90}Zr	0.28	97.80	0.95	0.65	0.49	<0.1
^{91}Zr	0.28	5.00	90.88	3.29	0.84	<0.2
^{92}Zr	0.28	2.86	1.29	94.57	1.15	0.14
^{94}Zr	0.51	1.67	0.42	0.76	96.93	0.22
^{96}Zr	0.46	9.19	2.02	27.20	4.22	57.36
^{93}Nb	0.28	only stable isotope				

Bassani et al.,[16] and the $(\alpha, {}^3\text{He})$ work of Bingham et al.[17] Reported studies of proton transfer reactions include the $(d, {}^3\text{He})$ work of Kavaloski et al.,[18] Preedom et al.,[19] Yntema,[20] and Ohnuma and Yntema,[21] and the $({}^3\text{He}, d)$ studies of Bassani et al.[22] The most notable lack of information on the single-nucleon transfer reaction is for proton stripping [i.e., $({}^3\text{He}, d)$ or (α, t)]. The only available data is the preliminary report of Ref. 22, and that work was confined to the $N = 50$ nuclei.

This paper reports the results from a study of the $({}^3\text{He}, d)$ reaction on all of the stable Zr isotopes and on the single stable isotope of Nb. These studies yield information on the shell-model distribution of protons in the ground states of ^{90,91,92,94,96}Zr and ^{93}Nb and aid in characterizing the properties of low-lying levels in the nuclei ^{91,92,93,95,97}Nb and ^{94}Mo.

The 50-neutron configuration which is filled through the $1g_{9/2}$ orbital is known to form a good major closed shell.[8,12] The nuclei of interest here have neutron numbers equal to or slightly in excess of 50. Any additional neutrons are observed to fill preferentially the $2d_{5/2}$ orbital; thus, the neutron configurations can be assumed to be reasonably simple. The 40 protons in the Zr isotopes, however, do not form a closed configuration,[18,19] and are expected to be distributed among the active orbitals of the $Z = 50$ major shell.

A stripping reaction such as $({}^3\text{He}, d)$ is a particularly sensitive tool for investigating small components of hole strengths within the ground state of a target nucleus. By using a series of targets with small differences in neutron and proton number, the systematic effects on the nuclear structure that result from adding neutrons or protons can be studied.

The experimental data consist of angular distributions of the deuterons resulting from the proton stripping reaction. They are analyzed, using the distorted-wave theory,[23–26] for the purpose of extracting spectroscopic information. This, in turn, is compared to the results of shell-model calculations.

II. EXPERIMENTAL DETAILS AND ENERGY SPECTRA

The reactions were produced by bombarding thin foils of isotopically enriched zirconium and natural niobium, prepared by the ORNL Isotopes Division, with ^{3}He ions from the Oak Ridge Isochronous Cyclotron. The beam energy was determined to ± 0.1 MeV by a 153° analyzing magnet. The emitted deuterons were detected in 50-μ Kodak NTB nuclear emulsions in a broad-range magnetic spectrograph.[27]

The energy of the incident ^{3}He ions was chosen to be well above the Coulomb barrier energy (about 16 MeV in this mass region), and low enough to achieve good absolute energy resolution. For the ^{91,92}Zr and ^{93}Nb reactions, the average beam energy for the various cyclotron runs was 30.9 MeV. For the ^{94,96}Zr reactions the beam energy was 24.7 MeV. The ^{90}Zr reaction was studied at both energies.

Aluminum absorbers were used in the focal plane of the spectrograph to eliminate unwanted tritons. Spectrograph entrance angles of ± 1.5 and ± 2.0 degrees were used and typical solid angles were of the order of 5×10^{-4} sr. Over-all resolution for the deuteron groups, limited by the target thickness, ranged from 30 to 55 keV. The nominal thicknesses and isotopic abundances of the targets are given in Table I.

In order to reduce uncertainties due to difficulties in accurate thickness determinations of these thin targets, as well as problems with accurate charge collection in the spectrograph scattering chamber, the product of integrated beam current and target thickness was

[16] G. Bassani, J. Picard, N. Saumier, and G. Souchere, J. Phys. Soc. Japan Suppl. 24, 649 (1968). Note added in proof. Now published as G. Bassani and J. Picard, Nucl. Phys. A131, 653 (1969).

[17] C. R. Bingham, M. L. Halbert, and R. H. Bassel, Phys. Rev. 148, 1174 (1966).

[18] C. D. Kavaloski, J. S. Lilley, D. C. Shreve, and N. Stein, Phys. Rev. 161, 1107 (1967).

[19] B. M. Preedom, E. Newman, and J. C. Hiebert, Phys. Rev. 166, 1156 (1968).

[20] J. L. Yntema, Phys. Letters 11, 140 (1964).

[21] H. Ohnuma and J. L. Yntema, Phys. Rev. 176, 1416 (1968).

[22] G. Bassani, J. Picard, and G. Souchere, J. Phys. Soc. Japan Suppl. 24, 649 (1968). Note added in proof. Now published as J. Picard and G. Bassani, Nucl. Phys. A131, 636 (1969).

[23] R. H. Bassel, R. M. Drisko, and G. R. Satchler, ORNL Report No. 3240 (unpublished).

[24] R. H. Bassel, Phys. Rev. 149, 791 (1966).

[25] G. R. Satchler, Nucl. Phys. 55, 1 (1964).

[26] G. R. Satchler, Lecture Notes for the 1965 Summer Institute for Theoretical Physics, University of Colorado, Boulder, Colorado, 1965 (unpublished).

[27] J. B. Ball, IEEE Trans. Nucl. Sci. NS-13, 340 (1966).
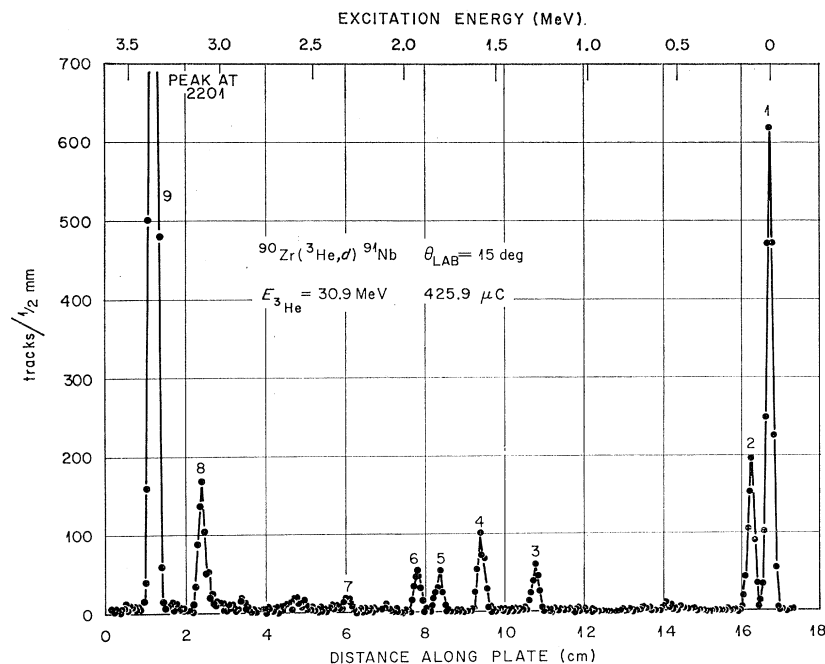
FIG. 1. Experimental spectrum of deuterons at 15° from the (^{3}He, d) reaction on ^{90}Zr at 30.9 MeV.

determined for each plate exposure from the ^{3}He elastic scattering detected by a monitor counter at a fixed scattering angle. Calibration of this monitor counter was accomplished by measuring the ^{3}He elastic cross sections with the spectrograph over a range of angles where the cross sections were well-known from previous data.[28] This method eliminated the need for precise determination of the scattering angle and solid angle of the monitor counter. The over-all uncertainty in the reaction cross sections, exclusive of counting statistics, is estimated to be 10–15%.

Figures 1–6 show the highest-energy deuteron groups from the (^{3}He, d) reaction on each of the targets at one typical scattering angle. Several adjacent plates were exposed in each run which extend the range of recorded excitation to about 10 MeV, but only the low-lying states are treated in this paper. These levels are numbered, in each figure, beginning with the ground state.

III. ANGULAR DISTRIBUTIONS AND SPECTROSCOPIC FACTORS

Angular distribution data for these reactions were taken over a range of scattering angles from about 6 to 30 deg. The specific angles were chosen to allow reliable identification of l-transfer values and extraction of spectroscopic factors. Exceptions to this are the data on the ^{93}Nb target where mixed l transfers are present, and the data on the ^{94}Zr target. In both of these latter cases, however, the data is sufficient to allow the extraction of the spectroscopic information of interest to the present study.

The experimental spectroscopic factors C^2S for given levels are determined by fitting the theoretically predicted angular distributions to the forward maximum of the experimental distributions and applying the expression

$$\sigma(\theta)_{\text{expt}} = 4.42[(2J_f+1)/(2J_i+1)]C^2S\sigma(\theta)\,(\text{JULIE}). \quad (1)$$

In this expression, J_i and J_f are the initial- and final-state spins and 4.42 is the normalization for the (^{3}He, d) reaction suggested by Bassel.[24] The theoretical angular distributions were calculated, in the local zero-range approximation, with the code JULIE.[29] Spin-orbit effects were included in the calculations.

The parameters used in the distorted-wave Born-approximation (DWBA) calculations are shown in Table II. The ^{3}He channel optical-model parameters are a set with a radius parameter of 1.14 F.[19,28] The deuteron parameters of Newman et al.[30] were used for the 31-MeV data, and those of Perey and Perey[31] for the 25-MeV data. The bound-state well depths are determined by requiring that the proton separation energy be an eigenvalue of the bound-state well.

In extracting spectroscopic factors, uncertainties in the DWBA calculations lead to an over-all uncertainty of order 30% in the absolute values of C^2S. Relative values of the spectroscopic factors are free from the largest sources of error in these calculations. The errors quoted for the normalized spectroscopic factors in Tables III–VIII reflect the statistical uncertainties in the measured cross sections and an estimate of the

[28] M. R. Cates, Ph.D. Thesis, Texas A & M University, 1969 (unpublished).

[29] R. M. Drisko (unpublished).
[30] E. Newman, L. C. Becker, B. M. Preedom, and J. C. Hiebert, Nucl. Phys. **A100**, 225 (1967).
[31] C. M. Perey and F. G. Perey, Phys. Rev. **152**, 923 (1966).
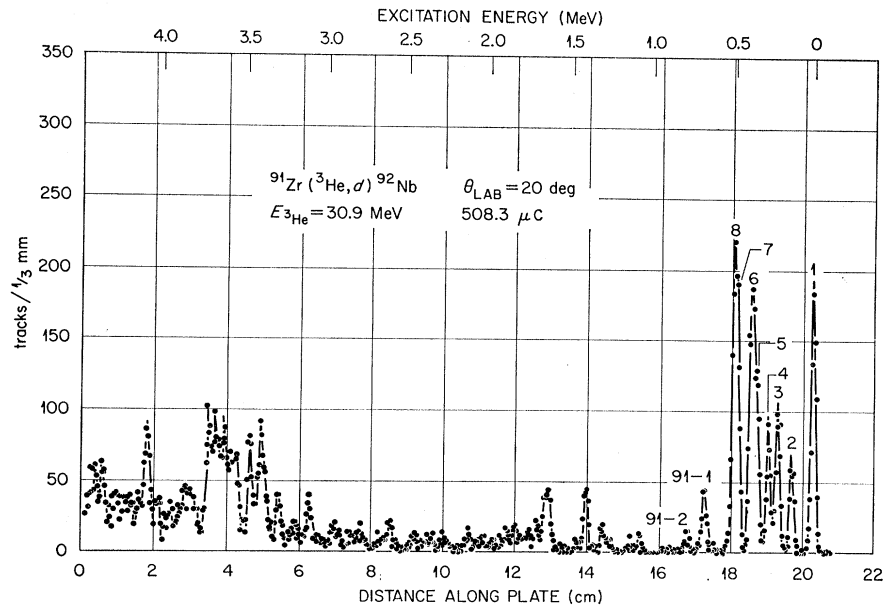
FIG. 2. Experimental spectrum of deuterons at 20° from the (^{3}He, d) reaction on ^{91}Zr at 30.9 MeV.

accuracy with which the DWBA calculation correctly predicts the relative n, l, j, and Q dependence of the reaction.

Since the major emphasis of this work is to study the proton structure of these isotopes, we are primarily interested in proton stripping into the shell-model orbitals that are being filled in this mass region. We expect the active orbitals to be the $1g_{9/2}$, $2p_{1/2}$, and possibly $2p_{3/2}$ and $1f_{5/2}$. Since the corresponding neutron levels are essentialy filled,[8,12] for l transfers of 1, 3, and 4 there should be no appreciable splitting of the proton strength due to isobaric spin considerations.[32,33]

At some excitation we expect to observe states arising from stripping into orbitals in the next major shell, e.g., the $2d_{5/2}$ orbital. Since the corresponding neutron orbitals are not completely filled, such stripping strength will be divided between the $T_<$ and $T_>$ states.

A. ^{90}Zr(^{3}He, d)^{91}Nb

The levels observed in ^{91}Nb, up to an excitation energy of 3.36 MeV, are listed in Table III. The angular distributions and comparison with the DWBA calculations are shown for the ground state ($l=4$) and 1.84 MeV state ($l=3$) in Fig. 7. The angular distributions for the four states observed to have $l=1$ character are shown in Fig. 8. The three low-lying states that we assign as $l=2$ transitions are shown in Fig. 9.

The ground state and first excited state for ^{91}Nb would seem to be well established as $\frac{9}{2}+$ and $\frac{1}{2}-$, respectively. Such an assignment is consistent with the interpretation of populating these states with this reaction by "stripping" a proton into the $1g_{9/2}$ and

$2p_{1/2}$ orbitals, respectively. The spectroscopic factors based on the DWBA predictions for these transfers are shown in Table III.

The higher lying states populated by $l=1$ stripping can be due to either $2p_{1/2}$ or $2p_{3/2}$ transfer. Spectroscopic factors for both possibilities are given in Table III. The results of this work cannot distinguish between the two possibilities. We can infer, however, that the higher $l=1$ states most likely arise from stripping protons into the $2p_{3/2}$ orbital. In particular, the states at 1.31 and 1.61 MeV have been observed in the ^{92}Mo(d, ^{3}He) reaction by Ohnuma and Yntema.[21] They observe both of these states with too much $l=1$ pickup strength to be consistent with $2p_{1/2}$ transfer. Their strong pickup strength and our relatively weak stripping strength is quite consistent with these two states being $\frac{3}{2}-$ states. The higher $l=1$ state seen in this work at 2.33 MeV is above the region of excitation covered in the (d, ^{3}He) work and no definite assignment can be inferred.

The state at 1.84 MeV is observed to have $l=3$ character and is ascribed to stripping a proton into the $1f_{5/2}$ orbital. This state is also reported in the (d, ^{3}He) studies with a large strength for $l=3$ pickup.[21] The observation of this state in the present work implies that the $1f_{5/2}$ orbital is not completely filled by the protons in the ^{90}Zr ground state. Since the $1f_{5/2}$ orbital is believed to lie deeper in the shell-model potential than the $2p_{3/2}$ orbital, the observation of $1f_{5/2}$ hole strength in ^{90}Zr supports the argument that some of the $l=1$ transfers should be due to $2p_{3/2}$ holes.

The states observed with $l=2$ stripping are assumed to arise from populating the $2d_{5/2}$ orbital. This strength is expected to be spread over many $T_<$ states in analogy with the results reported for the ^{89}Y(^{3}He, d) reaction[34,35]

[32] M. H. Macfarlane and J. B. French, Rev. Mod. Phys. 32, 567 (1960).

[33] J. B. French and M. H. Macfarlane, Nucl. Phys. 26, 169 (1961).

[34] G. Vourvopoulos, Ph.D. Thesis, Florida State University, 1967 (unpublished).

[35] G. Vourvopoulos and J. D. Fox, Phys. Rev. 177, 1558 (1969).

EXCITATION ENERGY (MeV)
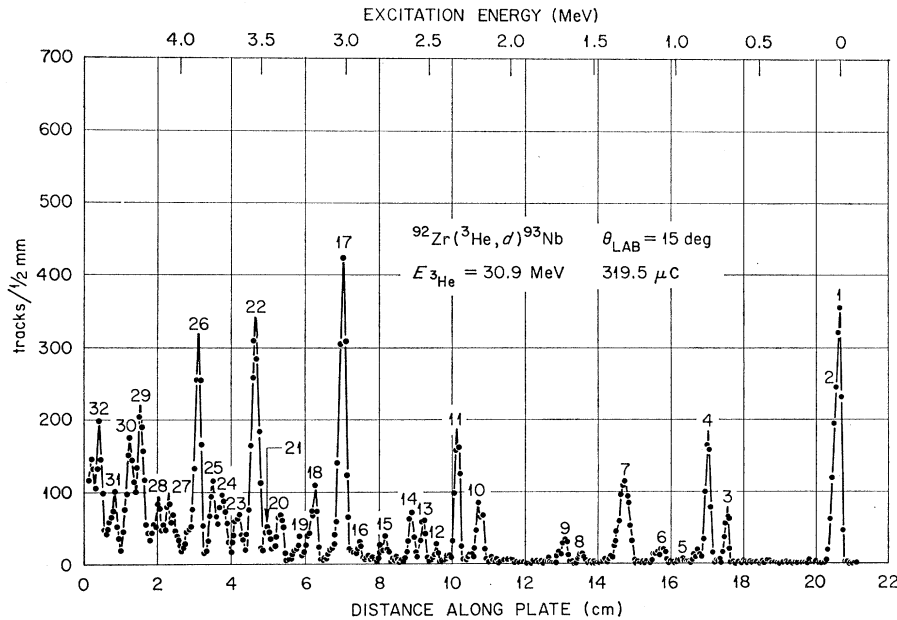
FIG. 3. Experimental spectrum of deuterons at 15° from the (^{3}He, d) reaction on ^{92}Zr at 30.9 MeV.

and only the lowest members are shown here. An analysis of the $l=2$ states observed in this reaction is the subject of another study.[36]

To facilitate comparison of our results with the shell model, we have also shown in Table III a set of renormalized spectroscopic factors. The renormalization is based on the following assumptions: (1) In the ^{90}Zr ground state, there is no appreciable population of proton orbitals above the $Z=50$ shell closure, (2) the ten holes in the ^{90}Zr proton configuration are distributed

only among the $1g_{9/2}$, $2p_{1/2}$, $2p_{3/2}$, and $1f_{5/2}$ orbitals, and (3) all the $2p_{1/2}$ strength is contained in the state at 0.104 MeV. Since we have already justified a $\frac{3}{2}-$ assignment for the second and third $l=1$ states, the main uncertainty is caused by the 2.33-MeV level. This state is only excited weakly and its assignment has no significant effect on the division of strength between $2p_{1/2}$ and $2p_{3/2}$. We favor assigning this state as $\frac{3}{2}-$, however, because this assignment gives a splitting between the $\frac{1}{2}-$ state and the center of gravity of the three $\frac{3}{2}-$ states of 1.55 MeV. This is in good agreement with a value of 1.51 MeV for the $2p_{1/2}$-$2p_{3/2}$ splitting observed in the ^{90}Zr(d, ^{3}He)^{89}Y reaction.[19]

The above assumptions, and the relationships for the
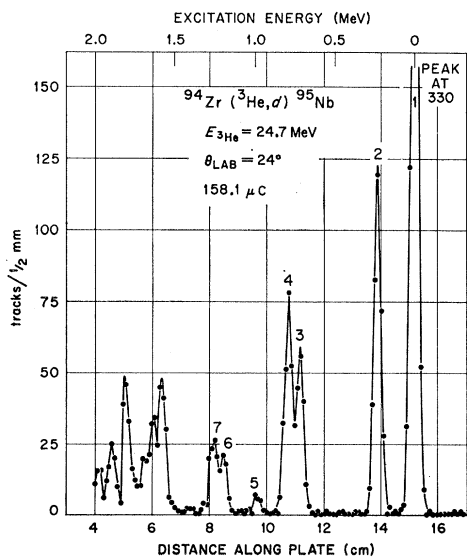
FIG. 4. Experimental spectrum of deuterons at 24° from the (^{3}He, d) reaction on ^{94}Zr at 24.7 MeV.

[36] G. Vourvopoulos, R. Shoup, J. D. Fox, and J. B. Ball, in *Nuclear Isospin*, edited by J. D. Anderson, S. D. Bloom, J. Cerny, and W. W. True (Academic Press Inc., New York, 1969), p. 205.
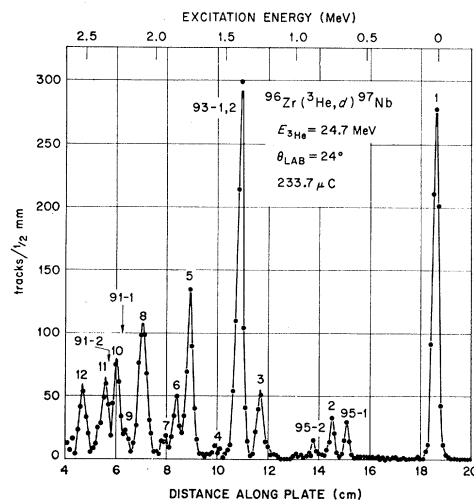
FIG. 5. Experimental spectrum of deuterons at 24° from the (^{3}He, d) reaction on ^{96}Zr at 24.7 MeV.
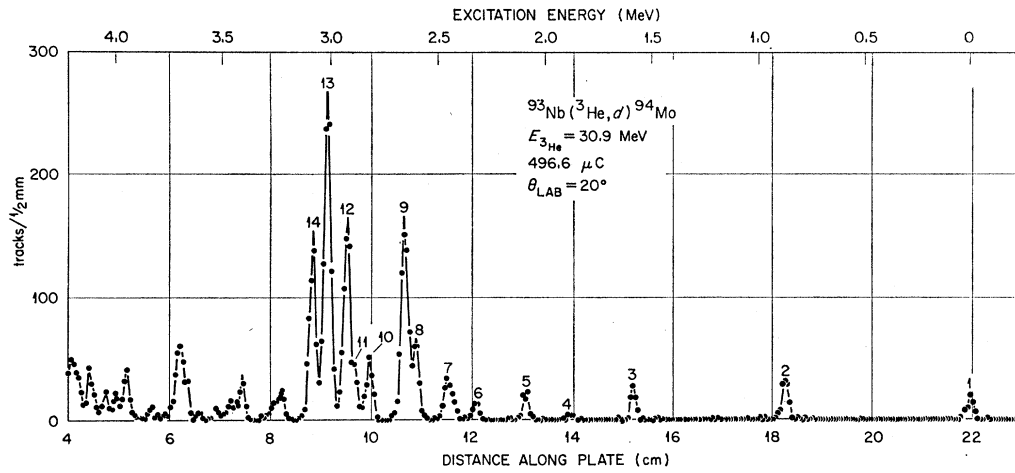
FIG. 6. Experimental spectrum of deuterons at 20° from the (^{3}He, d) reaction on ^{93}Nb at 30.9 MeV.

number of holes η in a given subshell,

$$\eta_j = (2J_i + 1)^{-1} \sum_f (2J_f + 1) C^2 S_f(j), \qquad (2)$$

lead to the renormalized spectroscopic factors of Table III. This renormalization is equivalent to changing the coefficient in Eq. (1) to a value of 5.59.

The preliminary spectroscopic factors of Bassani et al.[22] obtained from a similar DWBA analysis and renormalized in a similar manner, are in general qualitative agreement with those in Table III. The largest discrepancy occurs for their value of 0.3 for the 0.104 MeV state as compared to the 0.42±0.03 quoted here. No specific explanation for this disagreement is known. It should be noted, however, that we are deriving our spectroscopic factors by fitting the first maximum in the angular distribution. In the case of the $l=1$ levels, the DWBA calculation often fails to accurately predict

the correct relative magnitudes of the first and second maxima. If the first maximum is not observed, as is often the case for data taken with counters, the use of second maximum to determine the spectroscopic strength could lead to a value somewhat different than we would obtain.

To check on the consistency of the extracted spectroscopic factors, the ^{90}Zr reaction was also studied at 25 MeV. Angular distributions for the ground and first excited states are shown in Fig. 10. The parameters used

TABLE II. Optical-model parameters used in the DWBA calculations. The notation for the parameters is the same as that of Satchler.[a]

	^{3}He	d (34 MeV)	d (25 MeV)
V (MeV)	172.0	97.2	68.8
r_0(F)	1.14	1.12	1.033
a(F)	0.72	0.80	0.986
W (MeV)	17.0	0.0	0.0
W_D (MeV)	0.0	12.8	11.0
r_0'F	1.55	1.31	1.415
a'(F)	0.80	0.79	0.716
r_c (F)	1.40	1.30	1.30
V_s (MeV)	0.0	7.0	5.34
r_s (F)	...	1.12	1.033
a_s (F)	...	0.80	0.986

Bound state: $r_0 = 1.20$ F, $a = 0.65$ F, and $\lambda = 25$.

[a] G. R. Satchler, Nucl. Phys. A92, 273 (1967).

TABLE III. Levels observed in ^{91}Nb with the ^{90}Zr(^{3}He, d) reaction.

No.	Excitation energy (MeV)	l	J^π	C^2S	C^2S (norm)[a]
1	0.000	4	$\frac{9}{2}+$	1.10	0.87±0.04
2	0.104±0.005	1	$\frac{1}{2}-$	0.54	0.42±0.03
3	1.310	1	$\frac{1}{2}-$	0.12	
			$\frac{3}{2}-$	0.048	0.038±0.005
4	1.608	1	$\frac{1}{2}-$	0.19	
			$\frac{3}{2}-$	0.078	0.062±0.006
5	1.84±0.01	3	$\frac{5}{2}-$	0.058	0.046±0.005
6	1.96	2	$\frac{5}{2}+$	0.014	0.011±0.002
7	2.33	1	$\frac{1}{2}-$	0.041	
			$\frac{3}{2}-$	0.017	0.013±0.002
8	3.10	2	$\frac{5}{2}+$	0.048	0.038±0.005
9	3.36	2	$\frac{5}{2}+$	0.45	0.36±0.03
1[b]	0.000	4	$\frac{9}{2}+$	1.02	0.87±0.03
2[b]	0.103±0.005	1	$\frac{1}{2}-$	0.47	0.40±0.03

[a] Normalized to 10 holes in the $1g_{9/2}$, $2p_{1/2}$, $2p_{3/2}$, and $1f_{5/2}$ orbitals. Normalization factor $=0.79$ for 31-MeV data and 0.86 for 25-MeV data.
[b] 25-MeV data.

TABLE IV. Levels observed in ^{92}Nb with the ^{91}Zr(^{3}He, d) reaction.

No.	Excitation energy (MeV)	l	j_p	$(2J_f+1) \times C^2S$	$(2J_f+1)C^2S$ (norm)[a]
1	0.000	4	$\frac{9}{2}$	14.2	11.3±1.1
2	0.130±0.005	4	$\frac{9}{2}$	4.7	3.7±0.7
3	0.225	1	$\frac{1}{2}$	2.5	2.0±0.1
4	0.285	4	$\frac{9}{2}$	7.2	5.7±0.9
5	0.350	4	$\frac{9}{2}$	9.5	7.4±0.9
6	0.388	1	$\frac{1}{2}$	3.0	2.4±0.1
7	0.478	4	$\frac{9}{2}$	11.4	9.0±1.1
8	0.503	4	$\frac{9}{2}$	12.7	10.0±1.1
	1.09±0.01	1	$(\frac{3}{2})$	0.14	
	1.32	1	$(\frac{3}{2})$	0.20	
	1.42	1	$(\frac{3}{2})$	0.60	
	1.64	1	$(\frac{3}{2})$	0.72	
	1.67	1	$(\frac{3}{2})$	0.60	
	1.72	1	$(\frac{3}{2})$	0.39	

[a] Renormalized by the same factor as the ^{90}Zr data.

TABLE V. Levels observed in ^{93}Nb with the ^{92}Zr(^{3}He, d) reaction.

No.	Excitation energy (MeV)	l	J^π	C^2S	C^2S (norm)[a]
1	0.000	4	$\frac{9}{2}+$	0.97	0.79±0.04
2	0.029±0.005	1	$\frac{1}{2}-$	0.66	0.53±0.03
3	0.685	1	$\frac{1}{2}-$	0.24	
			$\frac{3}{2}-$	0.09	0.07±0.005
4	0.807	2	$\frac{5}{2}+$	0.07	0.06±0.003
5	0.97±0.01	1	$\frac{1}{2}-$	0.02	
			$\frac{3}{2}-$	0.008	0.006
6	1.08	4	$\frac{9}{2}+$	0.05	0.04
7	1.29	1	$\frac{1}{2}-$	0.17	
			$\frac{3}{2}-$	0.06	0.05±0.01
	1.33	(2)	$(\frac{5}{2}+)$	0.05	0.04
8	1.57	1	$\frac{1}{2}-$	0.07	
			$\frac{3}{2}-$	0.03	0.02
9	1.66	2	$\frac{5}{2}+$	0.01	0.008
	1.71	2	$\frac{5}{2}+$	0.007	0.006
10	2.18	2	$\frac{5}{2}+$	0.04	0.03
11	2.32	2	$\frac{5}{2}+$	0.07	0.06
13	2.52	(0)	...	...	
14	2.59	2	$\frac{5}{2}+$	0.03	0.02

[a] Normalized to 10 holes in the $1g_{9/2}$, $2p_{1/2}$, $2p_{3/2}$, and $1f_{5/2}$ orbitals. Normalization factor =0.81.

TABLE VI. Levels observed in ^{95}Nb with the ^{94}Zr(^{3}He, d) reaction.

No.	Excitation energy (MeV)	l	J^π	C^2S	C^2S (norm)[a]
1	0.00	4	$\frac{9}{2}+$	1.0	0.86±0.09
2	0.26	1	$\frac{1}{2}-$	0.39	0.34±0.03
3	0.73	1	$\frac{3}{2}-$	0.052	0.045±0.008
			$\frac{1}{2}-$	0.12	
4	0.80	1	$\frac{3}{2}-$	0.089	0.077±0.003
			$\frac{1}{2}-$	0.20	
5	0.99	3	$\frac{5}{2}-$	0.035	0.030±0.009
6	1.20	1	$\frac{3}{2}-$	0.025	0.022±0.002
			$\frac{1}{2}-$	0.057	
7	1.26	(3, 4)	...	...	

[a] Normalized to 10 holes in the $1g_{9/2}$, $2p_{1/2}$, $2p_{3/2}$, and $1f_{5/2}$ orbitals. Normalization factor =0.86.

in the DWBA analysis are included in Table II and the spectroscopic factors derived are also shown in Table III. Very good correspondence is seen between the results at the two incident energies.

It is apparent by inspection of the spectroscopic factors for the $l=4$, $l=3$, and $l=1$ states that the preponderance of the strength is contained in the ground and first excited states. If the upper $l=1$ states are all $\frac{3}{2}-$ states, their total spectroscopic strength is only about $\frac{1}{4}$ of that of the 0.104-MeV state.

TABLE VII. Levels observed in ^{97}Nb with the ^{96}Zr(^{3}He, d) reaction.

No.	Excitation energy (MeV)	l	J^π	C^2S	C^2S (norm)[a]
1	0.00	4	$\frac{9}{2}+$	1.13	0.95±0.05
2	0.74	1	$\frac{1}{2}-$	0.10	0.084±0.008
3	1.26	1	$\frac{3}{2}-$	0.10	0.084±0.008
			$\frac{1}{2}-$	0.24	
4	1.56	1	$\frac{3}{2}-$	0.01	0.008±0.002
			$\frac{1}{2}-$	0.03	
5	1.75	2	$\frac{5}{2}+$	0.21	0.18±0.02
6	1.85	2	$\frac{5}{2}+$	0.060	0.050±0.006
7	1.95	...	...	...	
8	2.09	2	$\frac{5}{2}+$	0.17	0.14±0.02
12	2.52	2	$\frac{5}{2}+$	0.08	0.07±0.01

[a] Normalized to 10 holes in the $1g_{9/2}$, $2p_{1/2}$, $2p_{3/2}$, and $1f_{5/2}$ orbitals. Normalization factor =0.84.

TABLE VIII. Levels observed in ^{94}Mo with the ^{93}Nb(^{3}He, d) reaction. The definite J^π values, shown for some of the levels, are taken from the decay scheme work of Aras et al.[a] In all cases, these assignments are consistent with the l transfers observed in the present work.

| No. | Excitation energy (MeV)[b] | l | J^π | $(2J_f+1)C^2S$ | | | |
				$1g_{9/2}$	$2d_{5/2}$	$2p_{1/2}$	$2p_{3/2}$
1	0.000	4	0+	2.97±0.15			
2	0.873	2, 4	2+	4.50±0.6	0.27±0.07		
3	1.582	2, 4	4+	2.03±0.45	0.49±0.14		
4	1.868	2, 4	2+	0.38±0.22	0.14±0.07		
5	2.08	4	(0)+	2.78±0.15			
6	2.295	2, 4	( )+	0.81±0.21	0.18±0.05		
7	2.422	2, 4	6+	2.54±0.9	0.34±0.14		
	(2.392)		2+				
	2.527	1	(3, 4, 5, 6)−			0.186±0.13	0.146±0.13
8	2.566	2, 4	( )+	4.35±0.75	0.18±0.13		
9	2.614	1	(3, 4, 5, 6)−			4.35±0.27	3.55±0.28
10	2.773	2, 4	( )+	4.14±0.40	0.24±0.10		
11	2.837	1	(3, 4, 5, 6)−			1.02±0.12	0.825±0.11
12	2.875	4	(8)+	17.1±0.9			
13	2.960	4	(8, 1)+	27.9±1.2			
14	3.026	1	(3, 4, 5, 6)−			3.66±0.27	3.10±0.27

[a] N. K. Aras, E. Eichler, and G. G. Chilosi, Nucl. Phys. A112, 609 (1968).
[b] All ±0.005.

B. ^{91}Zr(^{3}He, d)^{92}Nb

The states of particular interest to this study are the eight low-lying states seen in Fig. 2. Of these eight, six exhibit predominantly $l=4$ angular distributions and two show $l=1$ distributions. Spectroscopic factors for these states and a few of the observed higher excited $l=1$ levels are given in Table IV.

The six low-lying states populated by $l=4$ transfer are considered to be the multiplet of states arising from the coupling of the transferred $1g_{9/2}$ proton with the odd $2d_{5/2}$ neutron present in the ^{91}Zr ground state. These positive parity levels have been observed previously in neutron pickup reactions on ^{93}Nb.[11,37] The spin assignments are made on the basis of the earlier work. Within the limits of the rather large errors in the present work, caused by difficulty in quantitative separation of closely spaced weak levels, these results agree with the previous assignments.

The two low-lying $l=1$ states are strongly excited and presumably correspond to the coupling of a transferred $2p_{1/2}$ particle with the $2d_{5/2}$ neutron to form a 2−, 3− doublet. These states are not populated by the neutron pickup reaction and had not been reported previous to a preliminary report on the present work.[38] Because of the simple configuration ascribed to these states, their population by the (^{3}He, d) reaction should be very nearly proportional to $2J+1$. The two states show a very close correspondence to this ratio and are assigned spins on this basis.

It is assumed that the higher-lying $l=1$ states arise principally from $2p_{3/2}$ transfer and the spectroscopic factors given in Table IV are based on this assumption. These higher states do not necessarily exhaust the $l=1$ strength but the high level density precludes further analysis with the present resolution. A set of spectroscopic factors renormalized with the same factor as the ^{90}Zr data is also shown in Table IV.

TABLE IX. Fractional emptiness u_j^2 of the proton orbitals in the even Zr ground states.

Subshell	^{90}Zr	^{92}Zr	^{94}Zr	^{96}Zr
$1g_{9/2}$	0.86	0.83	0.86	0.95
$2p_{1/2}$	0.42	0.53	0.34	0.09
$2p_{3/2}$	0.11	0.14	0.14	0.09
$1f_{5/2}$	0.05	⋯	0.03	⋯

TABLE X. Single-particle centers of gravity relative to the ground state. Energies are in MeV.

Isotope	$1g_{9/2}$	$2p_{1/2}$	$2p_{3/2}$	$1f_{5/2}$
^{91}Nb	0.00	0.10	1.59	1.84
^{93}Nb	0.04	0.03	0.98	⋯
^{95}Nb	0.00	0.24	0.84	0.99
^{97}Nb	0.00	0.74	1.29	⋯

[37] R. K. Sheline, C. Watson, and E. W. Hamburger, Phys. Letters 8, 121 (1964).

[38] J. B. Ball and M. R. Cates, Phys. Letters 25B, 126 (1967).
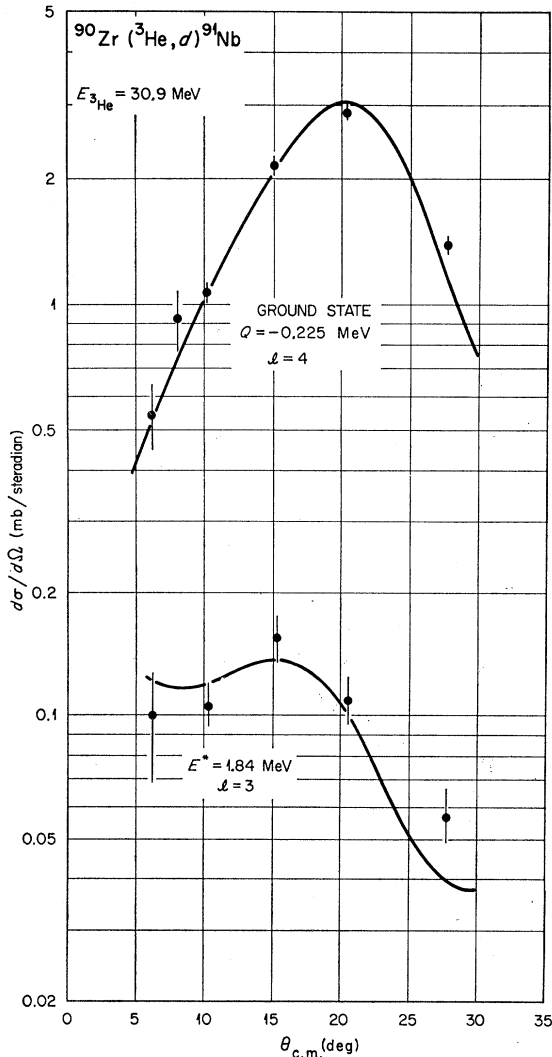
FIG. 7. Angular distributions for the ground and 1.84-MeV state from the ^{90}Zr(^{3}He, d) ^{91}Nb reaction at 30.9 MeV. The curves are the results of local zero-range distorted-wave calculations.

C. ^{92}Zr(^{3}He, d)^{93}Nb

The levels observed in this reaction up to 2.6 MeV are listed in Table V. Although the angular distributions are essentially identical to those shown previously, we show these to indicate the evidence for an excited state with $l=4$ character and our criteria for distinguishing between $l=1$ and $l=2$ transitions.

The ground and excited $l=4$ states are shown in Fig. 11. The states assigned $l=1$ and $l=2$ are shown in Figs. 12 and 13, respectively. In each of these latter figures one alternate l value is shown to indicate the expected difference between the $l=1$ and $l=2$ angular structure. All of the states seem to exhibit well-defined structure with the exception of the 1.33-MeV state (tentatively assigned as $l=2$) which was difficult to separate from the nearby $l=1$ state of comparable strength.

Also included in Table V are a set of spectroscopic

factors renormalized with the same criteria as the ^{90}Zr data. Again it is assumed that all of the $2p_{1/2}$ strength is contained in the transition to the first excited state. The renormalization coefficient obtained for the ^{92}Zr data is almost identical to that obtained for the ^{90}Zr data and lends some support to the rather arbitrary renormalization of the ^{91}Zr data.

The $l=2$ spectroscopic factors indicate that only a small amount of single-particle strength is represented in the lower $l=2$ states. They are all taken as $2d_{5/2}$ transitions although some of the states could be $2d_{3/2}$. Because the major portion of the expected $l=2$ strength is not observed in the low-lying states, it is likely that most of the $2d_{5/2}$ intensity is located above 2.6 MeV in excitation.
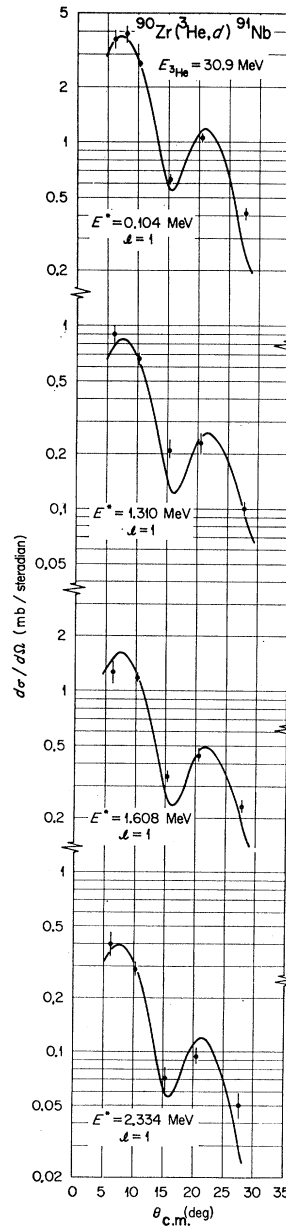
FIG. 8. Angular distributions for the $l=1$ states excited in the ^{90}Zr(^{3}He, d)^{91}Nb reaction at 30.9 MeV. The curves are the results of local zero-range distorted-wave calculations.

D. ^{94}Zr(^{3}He, d)^{95}Nb

This reaction was included primarily to aid in locating the impurity peaks in the ^{96}Zr reaction. Data were taken at only two scattering angles. A combination of these two angles and the impurity data from the ^{96}Zr target was sufficient to allow accurate spectroscopic factors for the ground and first excited state and reasonably certain l assignments to the higher excited states.

Further aid in identifying the higher levels is obtained by comparison with the reported ^{96}Mo(d, ^{3}He) results.[21] These authors report a strong $l=1$ transition
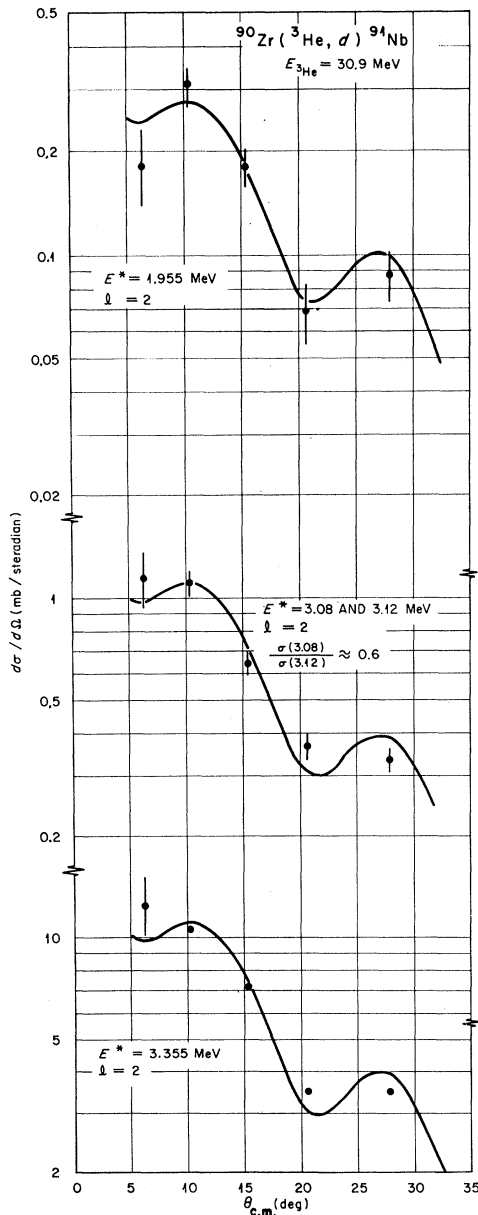
FIG. 9. Angular distribution for the $l=2$ states excited in the ^{90}Zr(^{3}He, d)^{91} Nb reaction at 30.9 MeV. The distribution in the center is that of the group comprising the 3.08- and 3.12-MeV levels. The curves are the results of local zero-range distorted-wave calculations.
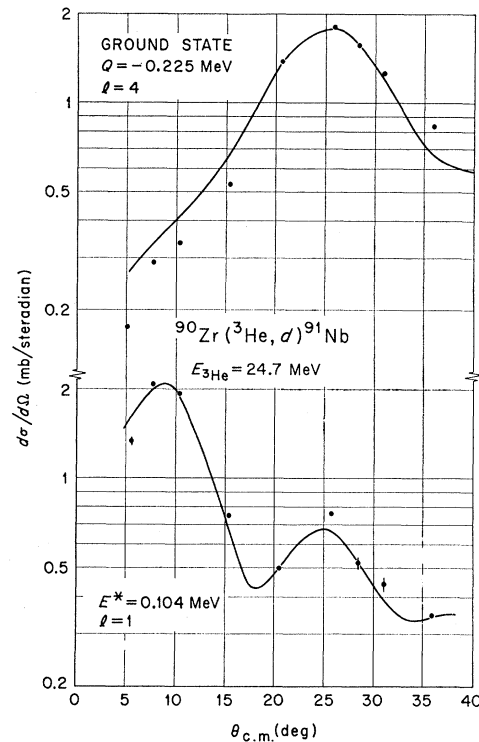
FIG. 10. Angular distributions for the ground and first excited state from the ^{90}Zr(^{3}He, d)^{91}Nb reaction at 24.7 MeV. The curves are the results of local zero-range distorted-wave calculations.

to a level at 0.77 MeV. We observe two $l=1$ levels, at 0.73 and 0.80 MeV, that would not have been resolved in their study. At least one of these levels must be $\frac{3}{2}-$ to account for the strong pickup strength but no firm assignments can be made to this pair. The pickup reaction shows a strong $l=3$ transition to a state at 0.98 MeV. This is consistent with the weak transition observed to this state in the present work if the state is assigned $\frac{5}{2}-$. The pickup study also reports a strong $l=1$ transition to a state at 1.22 MeV. Since we observe only one state in this region with $l=1$ transfer, and since it is weakly excited, this level is most probably a $\frac{3}{2}-$.

Data from the present study are summarized in Table VI. The somewhat larger errors on the spectroscopic factors reflect the poorer quality of the data for this reaction. The last column of the table shows a set of spectroscopic factors renormalized in the same manner as the ^{90}Zr and ^{92}Zr data. The renormalization constant of 0.86 is in good agreement with the factor of 0.84 required to relate the 25-MeV values for the ground and first excited states in ^{91}Nb (from the ^{90}Zr reaction) to renormalized 31-MeV values.

E. ^{96}Zr(^{3}He, d)^{97}Nb

The levels in ^{97}Nb up to an excitation of 2.52 MeV are presented in Table VII. The states observed include the $l=4$ ground state, three $l=1$, and several $l=2$ levels. The first excited state, at 0.74 MeV, is believed
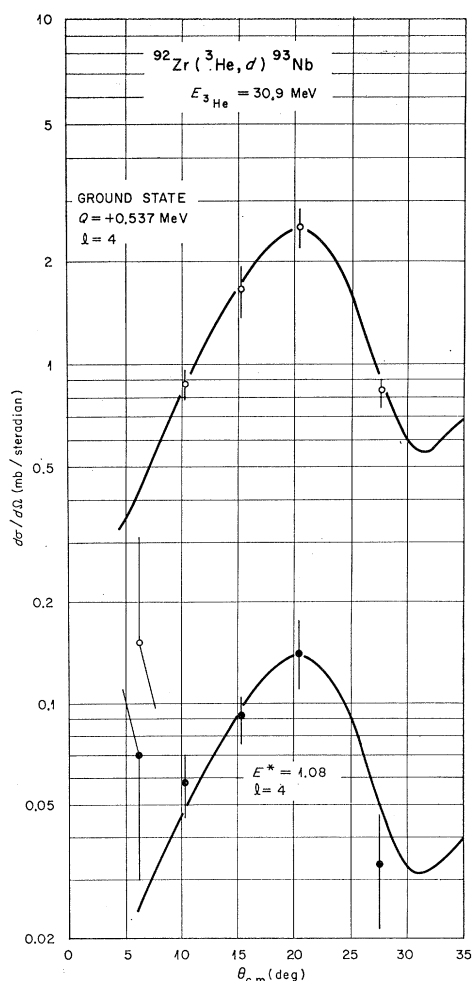
FIG. 11. Angular distributions for the two $l=4$ states excited in the ^{92}Zr(^{3}He, d)^{93}Nb reaction at 30.9 MeV. The curves are the results of local zero-range distorted-wave calculations.

F. ^{93}Nb(^{3}He, d)^{94}Mo

The angular distributions for the low-lying levels to 3 MeV in excitation, in ^{94}Mo, are shown in Figs. 14–16. Data at only four scattering angles have been taken, but with sufficient statistics to describe the general shape of the distributions.

The positive-parity levels in ^{94}Mo, depending on their spin, can be formed by mixtures of $l=0$, 2, and 4
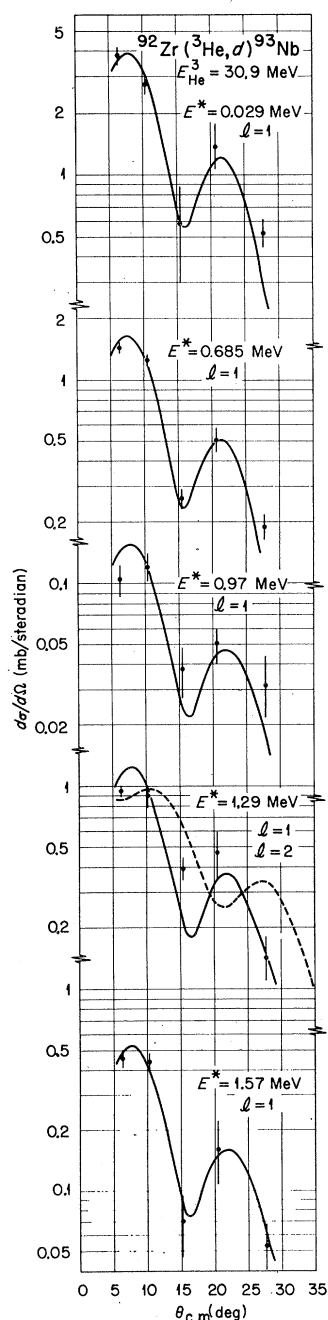
FIG. 12. Angular distributions for the $l=1$ states excited in the ^{92}Zr(^{3}He, d)^{93}Nb reaction at 30.9 MeV. The curves are the results of local zero-range distorted-wave calculations. The dashed curve, shown for comparison with the 1.29-MeV state, assumes $l=2$ transfer.

to be $\frac{1}{2}-$ and represents a much smaller portion of $2p_{1/2}$ single-particle strength than the $2p_{1/2}$ states in the other niobium isotopes studied. The ^{98}Mo(d, ^{3}He) reaction populates the 1.26-MeV level with more strength than allowed for $2p_{1/2}$ pickup. This state, fairly weakly excited in the present study, must then be $\frac{3}{2}-$. The $l=3$ state in ^{97}Nb observed by Ohnuma and Yntema[21] at 1.42 MeV, if excited by the stripping reaction, could not be seen because of strong isotopic impurity peaks near this excitation energy. Impurities in the target (see Table I) also prevent the analysis of possible ^{97}Nb states in the region between the 2.09 and 2.52 MeV. If the other two $l=1$ states are $\frac{3}{2}-$ levels, they would represent a $p_{3/2}$ hole component in the ^{96}Zr wave function similar in size to that in the ^{90}Zr nucleus. The $l=2$ states, as before, are thought to be $2d_{5/2}$ levels and show a considerable amount of strength at significantly lower excitation than for ^{90}Zr.

Renormalized spectroscopic factors are also shown in Table VII. The renormalizing constant of 0.84 is again quite consistent with the other 25-MeV results.

transitions. For the lower levels the predominant component is expected to be $l=4$ from $1g_{9/2}$ transfers. The $(^3\text{He}, d)$ reaction at this energy, on the basis of DWBA calculations, favors the $l=2$ transition by about an order of magnitude over the $l=4$ transition. For this reason, small portions of $l=2$ single-particle strength can significantly alter the shape of the angular distributions. Transitions with $l=0$ shapes, presumably from $3s_{1/2}$ protons, can also mix into 4+ and 5+ states.

The distributions in Fig. 14 appear to be reasonably pure $l=4$ transitions, but those in Fig. 15 show the influence of other l transfers. The composite shapes drawn through the data are sums of $l=2$ and $l=4$ predictions adjusted for a minimum in χ^2 given by

$$\chi^2 = \sum_i \left(\frac{A\sigma_g(i)+B\sigma_d(i)-\sigma_{\text{expt}}(i)}{\Delta\sigma_{\text{expt}}(i)}\right)^2, \qquad (3)$$

where A and B are the weightings of the theoretical differential cross sections σ_g and σ_d at each angle for the $1g_{9/2}$ and $2d_{5/2}$ proton transfers, and σ_{expt} and $\Delta\sigma_{\text{expt}}$ are the data and uncertainties at these same points.

The coupling of two $g_{9/2}$ protons will produce spins of 0, 2, 4, 6, and 8. A group of states in ^{94}Mo with these
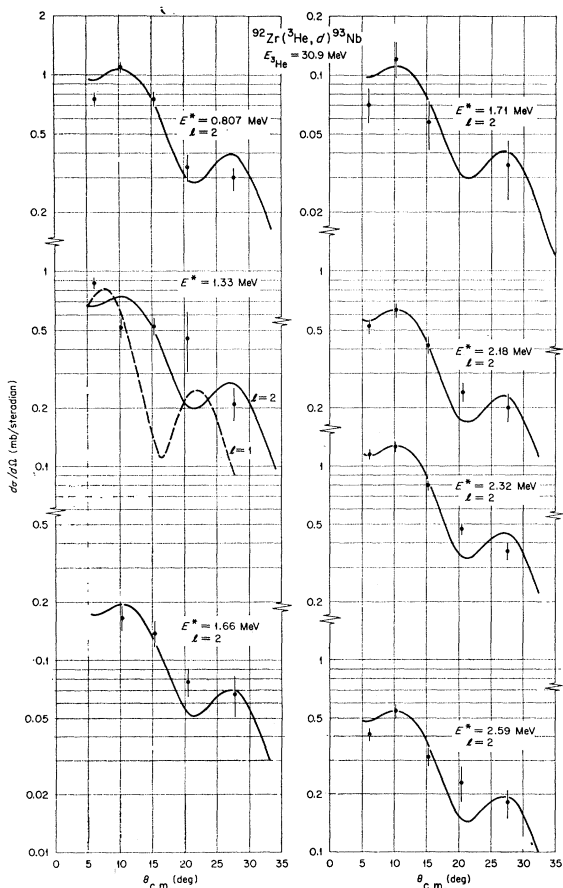
FIG. 13. Angular distributions for the $l=2$ states excited in the $^{92}\text{Zr}(^3\text{He}, d)^{93}\text{Nb}$ reaction at 30.9 MeV. The curves are the results of local zero-range distorted-wave calculations. The dashed curve compares the data with the prediction for an assumed $l=1$ transfer.
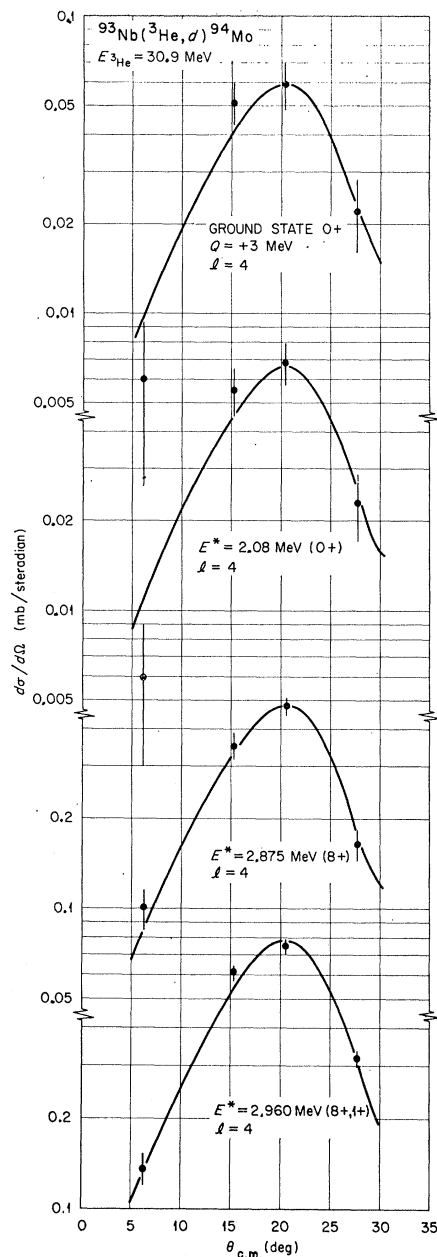
FIG. 14. Angular distributions for the predominantly $l=4$ transfers excited in the $^{93}\text{Nb}(^3\text{He}, d)^{94}\text{Mo}$ reaction at 30.9 MeV. The curves are the results of local zero-range distorted-wave calculations.

spins is expected to be populated by proton stripping. The 0+ and 8+ levels can be formed only by $l=4$ transfer. The 2+, 4+, and 6+ levels can have contributions from other l-transfers. As expected, the 0+ ground state in ^{94}Mo shows an $l=4$ distribution with no evidence of other contributing transitions. The 2+ states at 0.873 and 1.868 MeV display the effects of $l=2$ transitions, as do a number of other states.

Several negative-parity $(l=1)$ states were excited in the reaction (Fig. 16). Their presence in the spectra shows evidence for $p_{1/2}$ and possibly $p_{3/2}$ holes in the
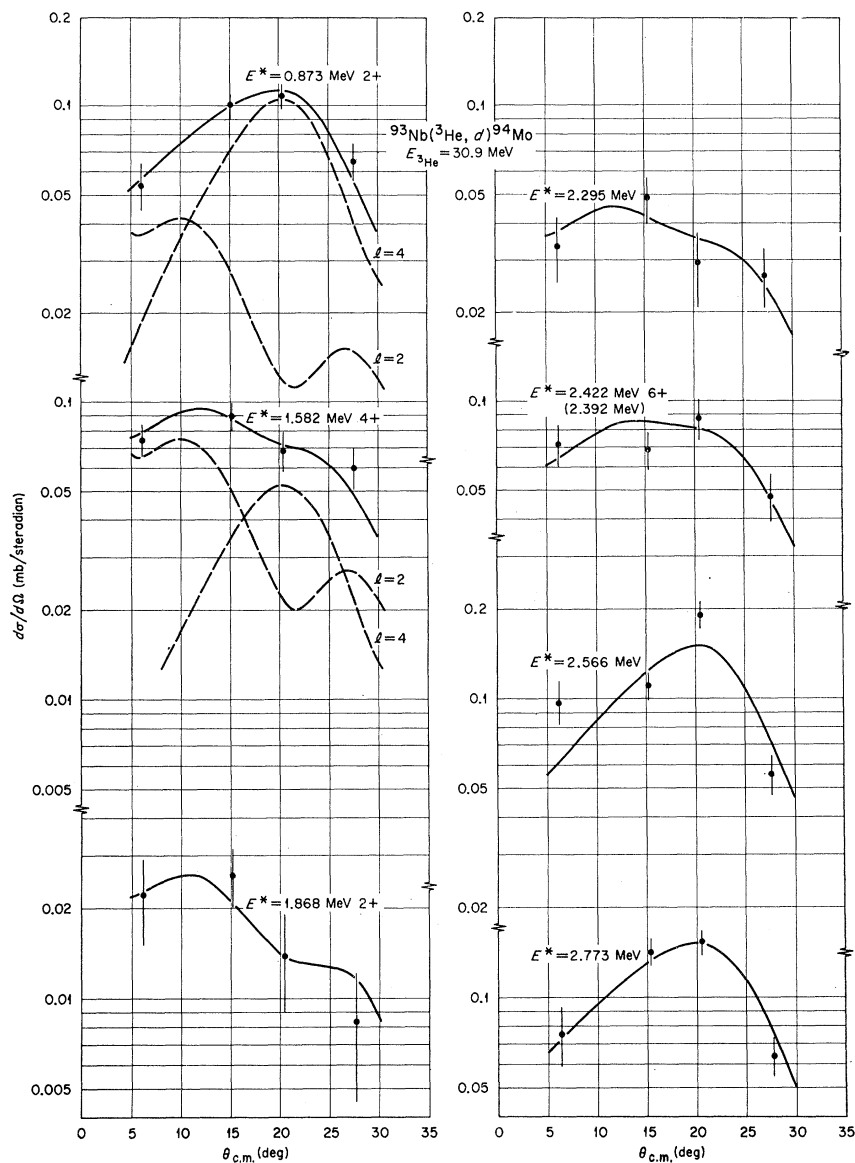
FIG. 15. Angular distributions for the positive-parity transitions from the ^{93}Nb(^{3}He, d)^{94}Mo reaction at 30.9 MeV. The solid curves are results of summing, incoherently, the appropriately weighted $l=2$ and $l=4$ calculations. The individual contributions are shown explicitly for the first two states as dashed curves.

proton configuration of the ^{93}Nb ground state. The addition of a $p_{1/2}$ proton to ^{93}Nb should lead to states with spins of 4— and 5—, while a $p_{3/2}$ proton would allow spins from 3— to 6—. In the group of states analyzed (to 3.03 MeV) four states are clearly $l=1$ in character, two of which (2.614 and 3.026 MeV) are quite strongly populated. These two strong states are good candidates for the 4—, 5— doublet expected from $p_{1/2}$ stripping.

In order to extract spectroscopic factors, all $l=4$ distributions have been taken as $1g_{9/2}$ transitions and all $l=2$ distributions as $2d_{5/2}$ transitions. Both the $2p_{1/2}$ and $2p_{3/2}$ values are computed for the $l=1$ levels. Because many final spins are unknown, the spectroscopic factors are written as $(2J+1)S$. No $l=0$ strength was noted among the positive-parity levels treated

here. Consequently, no attempt was made to estimate the $l=0$ contributions to the angular distributions. Table VIII, in similar fashion to the previous ones, summarizes the spectroscopic information.

An assessment using this spectroscopic information, of the number of $1g_{9/2}$, $2p_{1/2}$, and $2p_{3/2}$ holes in the ^{93}Nb proton configuration is very difficult because so few of the states can be identified as to final spin. In addition, some of the higher $l=4$ states, e.g., at 2.960 MeV, may contain $1g_{7/2}$ strength, or some of the $1g_{9/2}$ strength may be mixed into the unanalyzed upper levels.

An obvious feature of the positive parity states is that the $l=4$ strength is not distributed with a $(2J+1)$ weighting factor. For example, the sum of the $l=4$ strengths in the 2+ states at 0.873 and 1.868 MeV is not 5 times that of the ground state; nor is the 6+ state

at about 2.4 MeV excited any stronger than the ground state. A detailed comparison of these results with shell-model predictions will be given in Sec. V.

IV. SYSTEMATICS OF THE PROTON CONFIGURATION

A. Distribution of Proton Hole Strength

The spectroscopic factors of the preceding section yield information on the distribution of proton holes in the ground-state wave functions of the targets studied. In a stripping reaction the number of holes in the sub-shell is given by Eq. (2) and the fractional emptiness

Fig. 16. Angular distributions for the $l=1$ states excited in the ^{93}Nb$(^3$He, $d)^{94}$Mo reaction at 30.9 MeV. The curves are the results of local zero-range distorted-wave calculations.

TABLE XI. Comparison of the fractional emptiness of the proton orbitals in the ^{90}Zr ground state derived from the separation-energy form factors with those derived from the modified form factors. The separation and single-particle energies used in the calculation are also shown.

	Separation-energy procedure		Modified procedure	
Subshell	E_{sep}	$u_j{}^2$	$E_{\text{s.p.}}$	$u_j{}^2$
$1g_{9/2}$	5.27	0.86	6.16	0.87
$2p_{1/2}$	5.17	0.42	7.07	0.41
$2p_{3/2}$	3.66	0.11	8.51	0.09
$1f_{5/2}$	3.43	0.045	8.82	0.032

$u_j{}^2$ for the simple case of a zero-spin target is

$$u_j{}^2 = \eta_j/(2j+1) = \sum_f C^2 S_f(j), \qquad (4)$$

where η is the number of holes in the orbital with angular momentum j and $C^2 S_f(j)$ is the spectroscopic factor for states formed with that spin. The values of $u_j{}^2$, taken from the data for the even zirconium targets, are summarized in Table IX.

It is apparent from the table that the $1f_{5/2}$ and $2p_{3/2}$ proton orbitals are more nearly closed than the $2p_{1/2}$ orbital. Thus, it is reasonable that shell-model calculations considering only the $1g_{9/2}$ and $2p_{1/2}$ as active orbitals can account for many features of the low-lying states of these nuclei. It is also apparent that the hole strength in the deeper orbitals is not completely insignificant and we would expect, in some cases, to see deviations from the predictions of the simple model.

The center of gravity of the observed single-particle strength assigned to the different orbitals is shown in Table X. The systematics shown in Tables IX and X support each other in a very consistent fashion. The number of holes in the $p_{1/2}$ shell is directly related to the separation of the center of gravity of the $p_{1/2}$ and $g_{9/2}$ strength. As the separation decreases the number of $p_{1/2}$ holes increase and the $g_{9/2}$ becomes more filled. As the separation increases the $p_{1/2}$ shell becomes more filled and the $g_{9/2}$ becomes more empty. These systematics support the idea that the $2p_{1/2}$ orbital lies deeper in the shell model potential than the $1g_{9/2}$ orbital. The additional pairing energy of the $g_{9/2}$ orbital lowers its effective position close to that of the $p_{1/2}$ orbital for the lighter zirconium nuclei. There is a rather dramatic change as neutrons are added to the potential; the $2p_{1/2}$ is seen to move deeper in the potential than the $1g_{9/2}$. For ^{96}Zr the $2p_{1/2}$ level has become nearly full and the $1g_{9/2}$ almost empty.

The results shown in Tables IX and X are based on spectroscopic factors derived from DWBA calculations with bound state form factors chosen to yield the correct particle separation energies. This method is certainly open to question for stripping a particle into hole states representing small pieces of deeper lying orbitals. In

TABLE XII. Comparison of $1g_{9/2}$ and $2p_{1/2}$ spectroscopic factors from the ^{90}Zr(^{3}He, d) and (d, ^{3}He) reactions.

	$1g_{9/2}$	$2p_{1/2}$
S for (^{3}He, d)	1.10	0.54
No. of holes	11.0	1.08
Renorm. to 10 holes	9.11	0.89
u^2	0.91	0.44
S for (d, ^{3}He)	1.10	1.91
No. of particles renorm. to 2	0.73	1.27
v^2	0.07	0.63
u^2+v^2	0.98	1.07

this particular experiment we observed $p_{3/2}$ and $f_{5/2}$ proton stripping to levels at higher excitation than $p_{1/2}$ and $g_{9/2}$ levels, yet the $p_{3/2}$ and $f_{5/2}$ single particle orbitals are actually deeper in the shell-model potential. Thus our form factors for $p_{3/2}$ and $f_{5/2}$ transfer have the correct asymptotic behavior but correspond to single-particle energies inconsistent with our model.

To estimate the effect of our separation energy form factors on determining the absolute strength of the small hole components, we have repeated the DWBA calculations for the ^{90}Zr(^{3}He, d) reaction using form factors calculated according to a prescription suggested by Prakash and Austern.[39–41] The procedure may be summarized as follows: (1) The form factor of a Woods-Saxon well is calculated by requiring the solution to have the single-particle energy as an eigenvalue. (2) The particle separation energy is then used in this well and a *non*eigensolution is calculated. (3) At a radius, corresponding to the peak of the single-particle form factor, the inside and outside solutions are matched. (4) The new form factor is then renormalized to unity. The solution of the Schrödinger equation for the form factor was performed using a modified version of the code FANLFR2.[42] The form factors were then used in the code JULIE for the DWBA cross-section calculations.

The effect of the modified form factors on the deduced values for the fractional emptiness of the shell-model orbitals in ^{90}Zr is summarized in Table XI. Also shown in the table are the values taken for the separation energies and single-particle energies of the transferred protons. As expected, the only significant changes are observed for the $2p_{3/2}$ and $1f_{5/2}$ hole strengths. It is seen that the modified procedure says that the two deeper

orbitals are actually more nearly closed than indicated by the separation-energy procedure. The largest difference, about 30%, is for the deepest orbital, the $1f_{5/2}$. Since this is about the uncertainty generally quoted for absolute spectroscopic factors from the DWBA calculation, and since it is difficult to specify unambiguously the method of generating the modified form factors, we chose to quote the separation-energy results in Tables III–VIII. It would seem reasonable to conclude that these values for the $2p_{3/2}$ and $1f_{5/2}$ transfers represent upper limits.

A general conclusion for all the zirconium isotopes is that the $2p_{3/2}$ orbital appears to be about 90% filled for protons and the $1f_{5/2}$ orbital about 96% filled. From this standpoint then, it is not too surprising that a shell model assuming a ^{88}Sr core can account for many of the features of these nuclei.

B. Comparison with the (d, ^{3}He) Results

The Zr(d, ^{3}He) reaction studies by Preedom *et al.*[19] are of particular interest to the present work. By analyzing both stripping and pickup on the same nucleus, the sum of particle and hole strengths for each type of transition can be investigated to check for consistency of the analysis. That experiment was performed with 34-MeV deuterons, making the particle energies comparable to the present study. The DWBA analysis of both experiments therefore can be done using the same sets of parameters in the optical channels and the bound-state well, hopefully eliminating some uncertainties in the extraction of corresponding spectroscopic factors.

In a pickup reaction, the number of particles in a subshell is given by the total spectroscopic factor C^2S for transition into that level. The occupation probability for the subshell, denoted as v_j^2 is given by

$$v_j^2 = (2j+1)^{-1} \sum_f C^2 S_f(j), \qquad (5)$$

where $C^2 S_f(j)$ are the spectroscopic factors for the states formed by nucleon pickup from an orbital of angular momentum j. Obviously, for a consistent analysis, the sum of u_j^2, determined from the stripping

[39] A. Prakash, Ph.D. Thesis, University of Pittsburgh, 1966 (unpublished).
[40] A. Prakash, Phys. Rev. Letters **20**, 864 (1968).
[41] A. Prakash and N. Austern (to be published).
[42] J. K. Dickens and F. G. Perey, Oak Ridge National Laboratory Report No. ORNL-3858, 49, 1965 (unpublished). We are indebted to R. M. Drisko for supplying the modifications necessary for this analysis.

TABLE XIII. Coefficients for the $(2p_{1/2})^2$ component in the zirconium ground states.

Isotope	Present study	(d, ^{3}He) results[a]	Theory[b]
^{90}Zr	0.56±0.05	0.64±0.04	0.62
^{92}Zr	0.44±0.05	0.55±0.04	0.59
^{94}Zr	0.63±0.05	0.66±0.04	0.67
^{96}Zr	0.91±0.03	0.86±0.09	0.76

[a] Reference 19.
[b] Reference 43.

TABLE XIV. Comparison of experimental levels with shell-model predictions. Only levels populated by $l=1$ and $l=4$ proton transfer are included.

Nucleus	Experimental data			Calculation		
	J^π	E_{exc} (MeV)	C^2S	J^π	E_{exc} (MeV)	C^2S
^{91}Nb	$\frac{9}{2}+$	0.00	0.87	$\frac{9}{2}+$	0.00	0.93
	$\frac{1}{2}-$	0.10	0.42	$\frac{1}{2}-$	0.08	0.38
	$(\frac{3}{2})-$	1.31	0.04	$\frac{3}{2}-$	1.07	0
	$(\frac{3}{2})-$	1.61	0.06	...	...	...
	$\frac{5}{2}-$	1.84	0.05	$\frac{5}{2}-$	1.33	0
	...	...	...	$\frac{9}{2}+$	1.64	0.0005
	$(\frac{3}{2})-$	2.33	0.01	...	...	...
^{93}Nb	$\frac{9}{2}+$	0.00	0.79	$\frac{9}{2}+$	0.00	0.79
	$\frac{1}{2}-$	0.03	0.53	$\frac{1}{2}-$	−0.04	0.40
	$(\frac{3}{2})-$	0.69	0.07	$\frac{3}{2}-$	0.66	0
	$(\frac{3}{2})-$	0.97	0.006	...	...	...
	$\frac{9}{2}+$	1.08	0.04	$\frac{9}{2}+$	1.04	0.11
	$(\frac{3}{2})-$	1.29	0.05	...	...	...
	$(\frac{3}{2})-$	1.57	0.02	...	...	...
	...	...	...	$\frac{1}{2}-$	2.13	0.005
^{95}Nb	$\frac{9}{2}+$	0.00	0.86	$\frac{9}{2}+$	0.00	0.86
	$\frac{1}{2}-$	0.26	0.34	$\frac{1}{2}-$	0.08	0.33
	$\frac{3}{2}-$	0.73	0.05	$\frac{3}{2}-$	0.85	0
	$\frac{3}{2}-$	0.80	0.08			
	$\frac{5}{2}-$	0.99	0.03	$\frac{5}{2}-$	0.88	0
	...	...	...	$\frac{9}{2}+$	1.15	0.03
	$\frac{3}{2}-$	1.20	0.02	...	...	...
^{97}Nb	$\frac{9}{2}+$	0.00	0.95	$\frac{9}{2}+$	0.00	0.95
	$\frac{1}{2}-$	0.74	0.08	$\frac{1}{2}-$	0.23	0.24
	$\frac{3}{2}-$	1.26	0.08			
				$\frac{3}{2}-$	1.49	0
	$\frac{3}{2}-$	1.56	0.008			
	$\frac{5}{2}+$	1.75	0.18	...	...	...
^{94}Mo[a]	0+	0.00	2.4	0+	0.00	2.5
	2+	0.87	0.71	2+	0.84	0.83
	4+	1.58	0.18	4+	1.58	0.16
	2+	1.87	0.06	2+	1.83	0.94
				0+	2.19	0.06
	(0, 4)+	2.08	2.2/0.24			
				4+	2.21	0.83
				2+	2.60	0.03
	(6, 2)+	2.42	0.15/0.40			
				6+	2.68	1.23
	(5)−	2.61	0.31	5−	2.48	0.28
	...	...	...	4−	2.57	0.0001
	(4)−	3.03	0.32	4−	2.97	0.27

[a] The $l=4$ and $l=1$ spectroscopic factors for Mo have been renormalized with the same factor as the ^{90}Zr data.

reaction, and v_j^2, determined from the pickup reaction, should be unity.

As mentioned previously, ^{90}Zr is often treated with a model limiting the active protons to the $1g_{9/2}$ and $2p_{1/2}$ orbitals. Table XII shows a comparison of the (^{3}He, d) and (d, ^{3}He) results treated on this basis. The sum u^2+v^2 is quite close to unity for the $g_{9/2}$ shell, but too large for the $p_{1/2}$ shell. The implied coefficient of the

$(p_{1/2})^2$ component of ^{90}Zr is 0.56 for the stripping case and 0.63 for the pickup. This difference lies outside the statistical variations of the data, but is probably within the bounds of fluctuation for the DWBA calculations.

Such an analysis is rather strongly dependent on the accuracy of the $l=4$ spectroscopic factor because of the large change in the total number of holes with change in S. For example, if the spectroscopic factor for the $1g_{9/2}$

state from the $(^3\text{He}, d)$ reaction is increased by 10%, essentially exact agreement between the two reactions is obtained. The sum of u^2+v^2 is within 1% of unity for both $g_{9/2}$ and $p_{1/2}$ strength and the coefficient of the $(p_{1/2})^2$ wave function component becomes 0.60 for the stripping reaction. A variation of 10% in spectroscopic factor is certainly within the possible errors in the distorted-wave analysis of the present experiment.

A summary of an analysis of the $1g_{9/2}$ and $2p_{1/2}$ strength for all the even zirconium isotopes is shown in Table XIII. The $(p_{1/2})^2$ component in the wave function for the ground states of these nuclei, as deduced from the present stripping results, is compared with the results reported from the analysis of the $(d, ^3\text{He})$ reaction[19] on these same nuclei. The over-all agreement of the two sets of results seems quite satisfactory. The same trends are seen in both reactions and, except for ^{92}Zr, the two results are within the estimated experimental errors. The theoretical coefficients are taken from the shell-model calculations to be described in more detail in the following section. The over-all effect of the additional neutrons on the proton configuration is qualitatively reproduced by the shell-model results.

V. COMPARISON WITH SHELL-MODEL PREDICTIONS

Several authors have reported shell-model calculations for these nuclei that consider ^{88}Sr to be an inert core with the active protons distributed in the $1g_{9/2}$ and $2p_{1/2}$ orbitals. To date, no comparable calculations have been reported which include the effects of holes in the $2p_{3/2}$ and $1f_{5/2}$ orbitals. A comparison of the results for low-lying levels observed in this work with the predictions of a ^{88}Sr core shell-model calculation is shown in Table XIV. The shell-model results shown here are very similar to those reported in Refs. 4–6. The active protons are distributed in the $2p_{1/2}$ and $1g_{9/2}$ orbitals and the neutrons are confined to the $2d_{5/2}$ orbital. The major change is that the relative center of gravities of the $(\pi g_{9/2})(\nu d_{5/2})$ and $(\pi p_{1/2})(\nu d_{5/2})$ effective interactions have been adjusted to better reproduce the position of the negative parity states in ^{92}Nb and the ground-state $(p_{1/2})^2$ components of the previous section.[43]

For the ^{91}Nb nucleus, the calculation predicts only one $\frac{1}{2}-$ level. The predicted spectroscopic strengths for the $1g_{9/2}$ and $2p_{1/2}$ transfers are in good agreement with the experimental data. The excited $\frac{9}{2}+$ level calculated at 1.64 MeV is not observed experimentally, but this is not surprising in view of the extremely small predicted spectroscopic strength. A $\frac{3}{2}-$ state is predicted by the model from the coupling of one proton in the $2p_{1/2}$

[43] J. B. Ball, B. M. Preedom, M. R. Cates, and E. Newman, J. Phys. Soc. Japan Suppl. 24, 634 (1968).

orbital to the 2+ coupling of the remaining pair in the $1g_{9/2}$ orbital. Within the framework of our limited model, such a state cannot be excited by the stripping reaction and, consequently, it is indicated to have zero strength in the calculation. In the physical case, however, such a state will mix with any other nearby $\frac{3}{2}-$ states. If, for example, the $2p_{3/2}$ hole state falls in this region of excitation, these two states will be observed to share the $2p_{3/2}$ transition strength. Such a mechanism can account for the two $\frac{3}{2}-$ states observed at 1.31 and 1.61 MeV.

A very similar situation is seen for the nucleus ^{93}Nb. The calculation predicts an excited $\frac{9}{2}+$ level in excellent agreement with an observed $l=4$ transition to the state at 1.08 MeV. An excited $\frac{1}{2}-$ level is also predicted but, since it is calculated to lie well above the observed $l=1$ state and to have a very small strength, it is unlikely that any of the observed states correspond to this state. As in ^{91}Nb, a pair of $l=1$ states is observed in the region of the first $\frac{3}{2}-$ predicted by the calculation.

The excited $\frac{9}{2}+$ level predicted in ^{95}Nb is not seen experimentally but the predicted strength is much smaller than in the case of ^{93}Nb. Note that, although the spectroscopic strengths agree well, the calculated position of the $\frac{1}{2}-$ level is significantly lower than the observed excitation energy. This effect is more pronounced in the calculation for ^{97}Nb where the discrepancy between calculated and observed excitation energy of the $\frac{1}{2}-$ level is now 0.5 MeV. In the case of ^{97}Nb the predicted spectroscopic strength for the $\frac{1}{2}-$ level is also rather poorly predicted. It was seen in the previous section that these two quantities, excitation energy and transfer strength for the $\frac{1}{2}-$ are related. The difficulty in the model for ^{97}Nb is also reflected in the poorer estimation of the $(2p_{1/2})^2$ component for the ground state of ^{96}Zr (Table XIII).

The over-all agreement for the levels in ^{94}Mo is reasonably good. The $l=4$ spectroscopic strengths for the first 0+, 2+, and 4+ levels are very well predicted by the model. The lowest $l=1$ state is tentatively assigned 5− on the basis of comparison with the calculations. Although this state is somewhat closer in energy to a predicted 4−, this 4− is calculated to have a vanishingly small spectroscopic strength. A predicted higher-lying 4− has an energy and transfer strength in good agreement with the 3.03 MeV, $l=1$, level and hence the level is tentatively assigned 4−.

The most glaring discrepancy in the comparison of observed and calculated levels is the spectroscopic strength to the second 2+ in ^{94}Mo. The observation of this strength was of particular interest for comparison with the shell-model calculations and was the primary motivation for including this reaction in the present study. In a previously reported shell-model study of these nuclei,[3] the positive-parity levels were calculated assuming the ^{90}Zr core to be inert and restricting the

active protons to the $1g_{9/2}$ subshell. In that very restricted model, the lowest 2+ state in ^{94}Mo was calculated to derive most of its parentage from the 2+ coupling of the $2d_{5/2}$ neutron group and the second 2+ was due largely to the 2+ coupling of the $1g_{9/2}$ proton pair. The coupling of a transferred $g_{9/2}$ proton with the unpaired $g_{9/2}$ proton in the ground state of ^{93}Nb should then preferentially excite the second 2+ rather than the first 2+ state in ^{94}Mo.

As can be seen from Table VIII, the experimental observation is quite different from the simple predictions. The lowest 2+ is an order of magnitude more strongly excited than the second 2+. The predictions of the ^{88}Sr core model shown in the table, while an improvement over the ^{90}Zr core predictions, still retain the property of ascribing considerable $g_{9/2}$ proton 2+ coupling to the upper state and show very poor agreement with the experiment. It seems certain that enlarging the model basis to include both the $2p_{3/2}$ and $1f_{5/2}$ orbitals will continue the trend towards better agreement for the excitation of the 2+ states.

The $1g_{9/2}$ strength to the second 4+ state and first 6+ state is observed with at least a factor of 4 smaller strength than predicted. It is apparent that not all the $l=4$ strength has been observed in this experiment. Thus, it is not clear as to how much of the disagreement for the higher-lying states is due to experimental difficulties and how much due to the simplifying constraints placed on the calculations. The location of the remaining strength will probably require the stripping reaction to be studied at an energy more favorable to

$l=4$ transfer and with sufficient data points to allow detailed fitting.

VI. CONCLUSIONS

This study provides good evidence that the nuclei in the zirconium region have many nuclear properties amenable to a simple shell-model description. The general features of the systematics of the observed proton configurations are well reproduced by such calculations, as well as the single-particle strengths and positions of many of the low-lying states in the residual nuclei. The proton hole components of the $2p_{3/2}$ and $1f_{5/2}$ orbitals have been established in addition to confirming the $1g_{9/2}$ and $2p_{1/2}$ components previously obtained from proton pickup studies. The presence of significant transfer strength to the $2p_{3/2}$ and $1f_{5/2}$ orbitals, in the region of the low-lying levels, suggests that more detailed shell-model calculations would be useful in providing a better description of the wave functions for many of these states.